Is There A Stratospheric Radiative Feedback in Global Warming Simulations?

Yi Huang, Minghong Zhang, Yan Xia

Department of Atmospheric and Oceanic Sciences, McGill University, Montreal, Canada

Yongyun Hu

Department of Atmospheric and Oceanic Sciences, Peking University, Beijing, China

Seok-Woo Son

School of Earth and Environmental Sciences, Seoul National University, Seoul, South Korea

March, 2015

Corresponding author: Dr. Yi Huang, 805 Sherbrooke Street West, Montreal, Quebec, H3A 0B9, Canada. Email: Yi.Huang@mcgill.ca

Abstract

The radiative impacts of the stratosphere in global warming simulations are investigated using abrupt CO_2 quadrupling experiments of the Coupled Model Inter-comparison Project phase 5 (CMIP5), with a focus on stratospheric temperature and water vapor. It is found that the stratospheric temperature change has a robust bullhorn-like zonal-mean pattern due to a strengthening of the stratospheric overturning circulation. This temperature change modifies the zonal mean top-of-the-atmosphere energy balance, but the compensation of the regional effects leads to an insignificant global-mean radiative feedback (-0.02 ± 0.04 W m^{-2} K^{-1}). The stratospheric water vapor concentration generally increases, which leads to a weak positive global-mean radiative feedback (0.02 ± 0.01 W m^{-2} K^{-1}). The stratospheric moistening is related to mixing of elevated upper-tropospheric humidity, and, to a lesser extent, to change in tropical tropopause temperature. Our results indicate that the strength of the stratospheric water vapor feedback is noticeably larger in high-top models than in low-top ones. The results here indicate that although its radiative impact as a forcing adjustment is significant, the stratosphere makes a minor contribution to the overall climate feedback and its uncertainty in CMIP5 models.

Key words: Stratosphere, radiative feedback, CMIP5

1. Introduction

It is increasingly recognized that the stratosphere plays an important role in climate change. In addition to aspects such as the dynamical coupling to the tropospheric circulation (Gerber et al., 2012), the importance of the stratosphere is manifested in its impact on the radiation energy budget. Many stratospheric trace gas species, such as carbon dioxide, ozone, and water vapor, affect the radiation energy balance by interacting with the shortwave solar radiation and the longwave terrestrial radiation. Numerical experiments show that stratospheric contributions are critical for the climate system to maintain the balance of the top-of-the-atmosphere (TOA) radiation energy budget during transient climate change (Huang 2013a). For example, the magnitude of the overall time-varying stratospheric effect on the outgoing longwave radiation (OLR) can be comparable to that of the overall longwave cloud feedback, and the inter-model spread is as large as that of the overall non-cloud tropospheric feedback (Huang 2013b).

A climatic effect can be generally classified either as a forcing, which drives climate change, or a feedback, which determines the sensitivity (i.e., how strongly the climate system responds to a given forcing). With regard to the stratospheric radiative effect, especially that related to temperature variations, the conventional view is that it is a *forcing* effect that arises from the rapid temperature adjustment driven by the radiative cooling due to greenhouse gas perturbation (e.g., Hansen et al. 1997). Interestingly, even when greenhouse gas concentrations are identically prescribed, there may still be substantial inter-model differences in the temperature adjustment and thus in the overall strength of the adjusted radiative forcing (Zhang and Huang 2014). Hence, there is a need to explicitly assess the stratospheric radiative effect in climate feedback analysis.

On the other hand, some studies have hypothesized that stratospheric changes may be coupled with tropospheric and surface climates, and constitute a radiative *feedback* mechanism (Gerber et al., 2012; Dessler et al., 2013). For instance, the stratospheric overturning circulation, the so-called Brewer-Dobson Circulation (BDC), is projected to intensify in response to global warming (e.g., Butchart et al. 2006; Li et al. 2008; Manzini et al., 2014). This may affect both the stratospheric temperature, by enhancing the adiabatic cooling in the tropics and the warming in the extratropics, and the stratospheric water vapor, by modifying the troposphere-stratosphere transport (Feuglistaler et al. 2014). Stratospheric water vapor not only directly affects radiation budget by trapping outgoing radiation but also radiatively cools the stratosphere and thus may induce an indirect (Planck) effect. This process has been hypothesized as a stratospheric water vapor feedback (Forster and Shine 1999; Stuber et al. 2001; Joshi et al. 2010; Huang 2013b; Dessler et al. 2013).

It is of great interest to know whether a stratospheric feedback exists in the climate models and whether it affects climate sensitivity in a significant way. However, it is difficult to partition the overall effect to forcing and feedback during transient climate change (Huang 2013b). In this paper, we take advantage of the abrupt quadrupling CO_2 experiments of CMIP5 (Taylor et al. 2012) to separate the two effects, and focus on the effect that may constitute a feedback. In the following sections, we first explain the kernel method that is used to quantify the radiative effect of stratospheric temperature and water vapor responses. Then we examine the stratospheric responses and quantify the resulting feedback in the models in the quadrupling CO_2 experiment. To diagnose the possible causality, a set of experiments are conducted using the CAM5 model of the National Center of Atmospheric Research (NCAR). We then conclude the paper with a summary and discussion of the main findings.

2. Method

We measure a radiative effect, either forcing or feedback, by the radiative kernel method:

$$\Delta R_X = \frac{\partial R}{\partial X}\Delta X \tag{1}$$

Here $\frac{\partial R}{\partial X}$ is a set of pre-calculated radiative sensitivity kernels (Shell et al. 2008) and ΔX the change in a climatic variable, e.g., stratospheric temperature or water vapor concentration.

To separate the stratosphere from troposphere, we set the tropopause level as the lowest level where the temperature lapse rate is less than 2 K/km for a depth of more than 2 km in each grid box in each model following the standard definition of the World Meteorological Organization (WMO 1957). The stratospheric radiative effect is then integrated from the determined tropopause level to the model top. This analysis is done globally at every grid box and for each month.

The feedback parameter is defined as

$$\lambda_X = \frac{<\Delta R_X>}{<\Delta T_s>} \qquad (2)$$

where <…> denotes global average and T_s is the surface temperature. This parameter is of interest because it is directly related to the climate's overall sensitivity to radiative forcing.

The kernel-based feedback analysis procedure is well documented in the literature (Soden and Held 2006, Soden et al. 2008, and Shell et al. 2008). In addition, Huang (2013b) and Huang and Zhang (2014) advanced the method to account for forcing uncertainty in the procedure. The feedback analysis conducted here follows that of Huang and Zhang (2014).

Although the kernel method has been validated and mostly used for quantifying tropospheric radiative feedback, our tests show that it is an appropriate method for quantifying the stratospheric feedback as well. Firstly, using a radiative transfer model and based on different types of standard atmospheric profiles (McClatchey et al. 1972), the linearity of radiation response to stratospheric temperature and water vapor perturbations is verified. Fractional errors are less than 15% when approximating the radiation flux change caused by up to 20 K stratospheric temperature change by scaling the radiation flux change due to 1 K temperature perturbation, and are less than 25% when approximating the radiation change caused by quadrupling water vapor concentration by scaling the radiation change due to 20% water vapor perturbation (20-fold magnification in each case). It is worth noting that the temperature and water vapor changes that we are concerned with (see the following section) do not exceed these magnitudes. In addition, as found in previous studies (Huang et al. 2007; Zhang and Huang 2014), the stratospheric and tropospheric feedback is linearly additive. The difference between the sum of the radiation changes caused by tropospheric and stratospheric changes respectively and the radiation change caused by both changes simultaneously is generally within a few percent. Secondly, in order to assess the kernel uncertainty associated with model atmosphere and radiation code, we compare the feedback analysis results using two sets of kernels: one based on a NCAR model (Shell et al. 2008) and the other based on a Geophysical Fluid Dynamics Laboratory (GFDL) model (Soden et al. 2008). Although the GFDL model-based kernels do not cover the portion of the stratosphere above 30 hPa, the quantifications of ΔR_X (Eq. 1) for the portion below 30 hPa using the two sets of kernels are in good agreement, with a bias generally less than 10%. In summary, these test results suggest that the kernel-based linear decomposition can achieve a comparable accuracy for the stratospheric temperature and water vapor feedback as for the tropospheric feedback (Soden et al. 2008).

3. CMIP5 CO_2 quadrupling experiment

To isolate the feedback from forcing, we analyze the climate change simulated by the CMIP5 models in two idealized quadrupling CO_2 experiments: abrupt4xCO_2 and sstClim4xCO_2. In the abrupt4xCO2 experiment, the general circulation models (GCMs) are integrated for 150 years after the atmospheric CO_2 concentration is instantaneously quadrupled. A total of 11 models, as listed in Table 1, are available and included in this study. In the accompanying sstClim4xCO_2 experiment, the GCMs are integrated for 30 years with the sea surface temperature (SST) being fixed after the quadrupling. Among 15 models archived in the CMIP5, 11 models are used for the analysis and compared with the abrupt4xCO2 experiments (see Table 1).

3.1 Forcing adjustment

The change in a stratospheric temperature in the sstClim4xCO_2 experiment in relevance to its control run (the sstClim experiment) defines the forcing adjustment response. Figure 1 (top panel) shows that the stratospheric temperature adjustment settles very rapidly. In the sstClim4xCO_2 experiment, the stratospheric temperature drops considerably; most of the cooling is attained within a year and then the temperature steadies, allowing it to be considered a rapid adjustment of the forcing (Hansen et al. 1997). The multi-model global mean forcing adjustment, assessed according to Equation 1, is 1.9 W m^{-2}, compared to the instantaneous forcing of 5.4 W m^{-2} caused by the CO_2 quadrupling. We notice that the magnitude of temperature adjustment differs substantially across the models, which results in quantitative differences in their adjusted radiative forcing (Zhang and Huang, 2014). The inter-model spread (max-min) among 11 models amounts to 30% of the mean.

3.2 Stratospheric temperature feedback

In the abrupt4xCO_2 experiment when the SST is allowed to vary (Figure 1, bottom panel), stratospheric temperature continues to vary over the whole integration period (150 years) in many models. Because the radiative relaxation time in the stratosphere is short (as manifested by the temperature response shown in the top panel of Figure 1), the extended stratospheric temperature change cannot be understood as a forcing adjustment, but a response that likely relates to SST changes.

When the radiation anomaly caused by stratospheric changes in humidity or temperature, quantified using Equation 1, is plotted against the global annual mean surface temperature anomaly, significant correlation is observed in most models. This verifies a strong connection between the surface temperature and the stratospheric radiative effect under question, and justifies quantifying the stratospheric feedback using Equation 2, as commonly done for tropospheric feedback.

We first calculate the temperature response that can be considered as a feedback as the average of the last ten years (141- 150) of the abrupt4xCO_2 experiment minus forcing adjustment as quantified above in sstClim4xCO_2 experiment. Figure 2 shows the zonal-mean pattern of the feedback response of temperature and water vapor. A bullhorn pattern with positive changes extending from subtropical upper troposphere both upward and poleward is noticed in most of the models (see the mean of model ensemble, MME).

We then calculate the feedback parameter according to Equation 2 (see Table 1). The feedback response of stratospheric temperature consists of both positive and negative changes (Figure 2a). The bullhorn temperature response pattern leads to a distinct zonal mean feedback pattern especially in the mid-latitudes (Figure 3a). Although the feedback at every latitude zone is generally robust and different from zero, its global integration results in a weak global mean feedback parameter, λ_{Tst}. The multi-model ensemble mean of λ_{Tst} is -0.02 W m^{-2} K^{-1} with a standard deviation (STD) of 0.04 W m^{-2} K^{-1}, and a range from -0.09 W m^{-2} K^{-1}(MRI-CGCM3) to 0.04 W m^{-2} K^{-1} (IPSL-CM5A-LR). These results suggest that the global mean temperature feedback in the models is rather uncertain.

3.3 Stratospheric water vapor feedback

Figure 2b shows the feedback response of the stratospheric water vapor in the abrupt4xCO_2 experiment. The water vapor response reaches 4 times the unperturbed climatological values in many models. The feedback parameter, λ_{WVst}, quantified by the kernel method (Equation 1) has a multi-model mean value of 0.02 W m^{-2} K^{-1} and a standard deviation of 0.01 W m^{-2} K^{-1} (Table 1). It is interesting to note that because the OLR sensitivity to water vapor ($\frac{\partial R}{\partial q}$) changes sign from lower to upper stratosphere, a uniform moistening in the stratosphere would lead to a small overall radiative effect after compensation, such as in tropical regions (see Figure 3b).

When grouping the models according to their model top height, we find that the high-top (higher than 1 hPa) ones show noticeably stronger water vapor feedback (see Table 1). From the water vapor response pattern (Figure 2b), it is evident that the high-top models tend to simulate a relatively stronger lower stratospheric moistening in the extratropical regions. This leads to a substantial (>0.2 W m^{-2} K^{-1}) feedback in these regions (Figure 3b).

It is worth noting that stratospheric water-vapor feedback parameter shown in Table 1 is an order of magnitude smaller than the value reported by Dessler et al. (2013): 0.3 W m^{-2} K^{-1}. A few reasons may explain the difference. Firstly, the feedback evaluated here is defined with respect to the TOA radiation flux while that of Dessler et al. is evaluated at the tropopause. Stratospheric water vapor increases, by itself, would induce a greater change in downwelling radiation at the tropopause (R_1) than in the upwelling radiation at the TOA (R_2). This is because R_1 is more sensitive to the stratospheric emissivity (ε) increase than R_2. Consider a two-layer (troposphere and stratosphere) grey-atmosphere model, $\partial R_1/\partial \varepsilon$ equals σT_1^4, which is the blackbody emission at the stratospheric temperature T_1, while $\partial R_2/\partial \varepsilon$ equals $\sigma T_2^4 - \sigma T_1^4$, which is the difference between the blackbody emission at the equivalent troposphere-surface temperature T_2 and that at the stratospheric temperature T_1. It can be shown that $T_2^4 - T_1^4 < T_1^4$ given that the stratosphere is at radiative equilibrium and absorbs solar radiation. Secondly, the water vapor feedback given in Table 1 is measured by the kernel method (Eq. 1) and reflects only the emissivity effect of water vapor but not the indirect effect through stratospheric cooling. The subsequent stratospheric cooling (decrease in T_1) due to the radiative cooling caused by water vapor, however, will damp the emissivity effect on R_1 but enhance the effect on R_2. If the stratosphere adjusts to a new radiative equilibrium, the overall changes at the tropopause and at the TOA need to be balanced and thus the combined effect would be equal no matter whether it is evaluated at the TOA or tropopause. This means that the sum of water vapor and temperature radiative effects by the end of the abrupt4xCO2 experiment (when it approaches equilibrium), as given by Table 1, has appropriately accounted for the combined water vapor radiative effects.

3.4 Combined feedback

The above results indicate that the stratosphere has a sign-uncertain temperature feedback but a weak positive water vapor feedback. Adding the two effects yields a wide range of feedback strengths with a minimum of -0.06 W m^{-2} K^{-1} and a maximum of 0.07 W m^{-2} K^{-1}. As a result, the MME is nearly zero, with a STD of 0.04 W m^{-2} K^{-1} (Table 1). Although the global mean feedback is insignificant, stratospheric changes play a non-negligible role in local radiative feedback especially in extratropics (see Fig. 3).

To verify the feedback values obtained above using the differencing method (Equations 1 and 2), we also calculate the feedback parameters using a regression method, by regressing the global annual mean radiation anomalies in years 21-150 in the abrupt4xCO2 experiment to the surface temperature anomalies. The results obtained from the two methods are generally in agreement (see Table 1). The only noticeable discrepancy in the CCSM4 model is due to weak linear relationship between the stratospheric temperature-caused radiation anomaly and surface temperature anomaly (and thus greater regression uncertainty).

4. Cause of local stratospheric feedback

4.1 Temperature feedback

The analysis above indicates that the stratospheric temperature feedback is locally significant in the extratropics (Figs. 2a and 3a). The stratospheric temperature response shown in Figure 2a consists of both positive and negative changes. In general, the positive signals emerge from both sides of the subtropical tropopause region and extend poleward and upward in both hemispheres. This pattern of warming, looking like bull horns, does not resemble the temperature change that is caused by stratospheric moistening, which would be uniformly negative (e.g., Forster and Shine 1999). Instead, one can draw similarities between the feedback temperature response here and the temperature changes in many of the global warming experiments (e.g., Son et al. 2009), which suggests a common cause of the bullhorn-like feedback response of the stratospheric temperature.

We find that the bull horns-like temperature change pattern between 60°S and 60°N is very well correlated with the anomaly of the residual vertical velocity w^* (see Andrews et al 1987, Eq. 3.5.1b for definition) in the stratosphere (compare Figs. 4a and b). The increases of upwelling in the deep tropics and downwelling in the extropical regions, as shown in Figure 3b, particularly indicate strengthening of the BDC in the quadrupling CO_2 experiment as in the scenario integrations (e.g., Butchart et al., 2006; Manzini et al., 2014). The consequent adiabatic cooling and warming largely explain the bullhorn pattern in the stratospheric temperature change. This result suggests that the peculiar stratospheric temperature feedback response likely results from the strengthening of the BDC.

To verify that it is the SST-driven circulation change that gives rise to the bullhorn-like temperature feedback response in the stratosphere, we conduct the following experiment using CAM5 (Neale et al. 2010). The model is integrated from 1960 to 2007 with greenhouse gas concentration fixed at 1960 value but with time-varying historical SST values. Four ensemble runs are done. Figure 4c shows that this experiment reproduces the bullhorn-shaped temperature response pattern seen in the quadrupling CO_2 experiment fairly well (compare Figs. 4a and 4c). Although temperature trend in the Southern Hemisphere high latitudes is different, it is not statistically significant.

We diagnose the temperature tendency terms ($\frac{dT}{dt}$, T: temperature; t: time) in the CAM5 simulations, including those caused by dynamics (heat advection) and physics (the physical parameterizations of longwave and shortwave radiative heating, moist processes, vertical diffusion, deep convective detrainment and orographic gravity wave drag, etc). We find that the temperature tendency caused by the resolved dynamics, as opposed to the parameterized physics, accounts for the bullhorn-shaped temperature pattern. The pattern caused by the physics is dominated by radiative cooling, which is spatially uniform, as shown by previous studies (Forster and Shine 1999), and does not explain the bullhorn-shaped pattern. In comparison, the pattern caused by the dynamics (Figure 4 d) is also bullhorn-shaped and has a strong spatial correlation with the overall temperature trend pattern (correlation coefficient: 0.95). Moreover, the dynamically-caused temperature change pattern is well correlated with the anomalous residual vertical velocity w^* between 60°S and 60°N. The spatial correlation between the two variables is -0.54; the temporal correlation between the annual mean anomalies of the two variables at 50hPa averaged over the tropics (30°S-30°N) is -0.80. These results affirm that surface warming causes dynamics adjustment (BDC strengthening) in the stratosphere, which then leads to the distinct temperature change pattern.

It is important to note that the positive and negative temperature changes caused by the stratospheric circulation changes have compensating radiative effects over the globe. Using the kernel approach (Eq. 1) the global-mean feedback effect due to the dynamical term (Figure 4d) is calculated to be -0.01 W m^{-2} K^{-1}. This affirms that the dynamical heating/cooling does not lead to a significant feedback in the global-mean surface temperature.

4.2 Water vapor feedback

Unlike tropospheric water vapor variations, which can be largely explained by tropospheric temperature change and conservation of relative humidity, stratospheric water vapor is not controlled by local temperature. The water vapor and temperature change patterns (Figure 2) in the abrupt4xCO2 experiment bear no similarity in the stratosphere.

Figure 2 b shows that in most models the most noticeable stratospheric water vapor increase occurs in the lowermost stratosphere that is adjacent to the tropical upper troposphere region where the atmospheric moistening is maximized. This suggests that the stratospheric moistening is through mixing (e.g., isentropic) that transports water from tropical upper troposphere to lower stratosphere. Indeed, the global mean specific humidity in the lowermost stratosphere (above tropopause and below 70 hPa) and the tropical mean (30°S–30°N) upper tropospheric specific humidity (UTH) averaged in a 100 hPa layer below tropopause are strongly correlated. Table 2 shows that the correlation between the annual anomalies of the two variables in every model is greater than 0.9 (many close to 1).

The UTH control of the overworld stratosphere (above 70 hPa) is noticeably weaker (see Table 2). For this region, it is expected that the ascent strength of the BDC and the temperature at tropical cold point tropopause (CPT) also influence the stratospheric humidity (Gettelman et al. 2010, Feuglistaler et al. 2014). Similar to what is found by Dessler et al. (2014), we find strong anti-correlation (-0.81) between the residual velocity w^* and the CPT temperature, which indicates that the two control factors have degenerated to one (with compensating effects). We correlate the annual anomalies of the CPT temperature and the stratospheric specific humidity in each model and find significant correlation in some models. In comparison, the specific humidity in both lowermost and overworld stratosphere is better explained by the UTH, except for the MIROC5 model. We also conduct a multiple regression of the stratospheric humidity change against both variables: UTH and CPT. We find they together can explain most of the stratospheric water vapor change in most models, except for the overworld stratosphere in the INMCM4 model.

Finally, with regard to the inter-model differences in these variables, we find high correlation between the global mean overall stratospheric water vapor change and the tropical upper tropospheric water vapor change (correlation coefficient: 0.86), and the tropical CPT temperature (0.67), respectively. In summary, these results suggest that the moist increase in the lowermost stratosphere can be mostly attributed to mixing of upper tropospheric water vapor, while that in the overworld is also affected by changes in BDC strength and in tropical tropopause temperature.

5. Discussion and conclusions

We analyze the stratospheric responses in climate models that can be considered as a feedback to surface warming. The GCMs examined have a stratospheric temperature feedback ranging from -0.09 to +0.04 W m^{-2} K^{-1} and a weaker water vapor feedback from 0.01 to 0.03 W m^{-2} K^{-1}. The sum of the two effects ranges from -0.06 to 0.07 W m^{-2} K^{-1} with almost zero multi-model ensemble mean value. The high-end feedback magnitudes suggest that the stratosphere may have a non-negligible effect on climate sensitivity. The considerable range of the feedback values indicate that this feedback mechanism is poorly quantified in the models.

The overall climate feedback of the same CMIP5 models analyzed here amounts to -1.4±0.4 W m^{-2} K^{-1} (MME and STD, see Zhang and Huang, 2014). In comparison, the stratospheric feedback makes considerably less contribution to the overall climate feedback and its spread in these models. However, we note that the stratospheric adjustment, i.e., the rapid stratospheric temperature change that is induced by CO_2 cooling and is not related to surface warming, has a much more significant impact on the radiation energy budget (a MME of 1.9 W m^{-2}, in comparison to a 5.4 W m^{-2} instantaneous forcing of quadrupling CO_2). It can be concluded that the significant inter-model spread of the overall stratospheric radiative impact as noticed by Huang (2013b) can be mostly attributed to forcing adjustment.

We also note that the results here do not exclude the possibility of stratospheric feedback caused by mechanisms other than water vapor and temperature variations. For instance, Zhou et al. (2014) find a non-negligible cirrus cloud feedback in short-term climate variations in observational data (a fraction of which may be related to clouds above the tropopause and thus be considered a stratospheric feedback), although this feedback is insignificant in GCM global warming experiments (Zelinka et al., 2012).

With regard to the cause of stratospheric feedback, we find that the strengthening of the BDC explains the stratospheric temperature feedback. The circulation change causes the temperature change through both dynamical (via adiabatic heat advection) and radiative (via changing stratospheric water vapor) heating. These two mechanisms are characterized by distinctive zonal mean temperature change patterns. The dynamical heating pattern resembles the shape of bullhorns while the radiative heating pattern is much more uniform. This suggests that it should be possible to attribute the overall temperature change in both simulations and observation records to the two mechanisms based on these distinctive spatial signatures, which shall be investigated in future work.

Unlike temperature feedback, stratospheric water vapor shows positive feedback in all experiments. The stratospheric water vapor response largely results from transported moisture from the tropical upper troposphere through mixing, but is also modulated by cold point temperature as well as BDC strength. It warrants further research to clarify how different mechanisms (e.g., ascent strength vs. tropopause temperature) control the stratospheric water vapor change in a warming climate, at least in the models. It should be borne in mind that not all 11 CMIP5 models included in this analysis fully resolve the stratosphere. The high-top models seem to have a stronger water vapor feedback (see Table 1) and this can be attributed to the relatively stronger extropical lower stratospheric moistening, the effects of which are also stressed by Dessler et al. (2013).

Although the net effect of global-mean stratospheric temperature and waver vapor feedback is small, we find that stratospheric changes may be important for local radiative feedback. A significant positive feedback is found in the extratropics. This could effectively change meridional temperature gradient in the troposphere. Since the circulation is sensitive to temperature gradient change in addition to temperature change itself, this local radiative feedback can affect circulation in certain regions. This potential link between stratospheric feedback and tropospheric climate change needs to be explored in future study.

Acknowledgements

We thank three anonymous reviewers whose comments helped improve the quality of the paper. Y. Huang and MZ are supported by a Discovery grant form the National Science and Engineering Research Council of Canada (RGPIN418305-13). YX is supported by a postdoctoral fellowship of Fonds de recherché du Québec- Nature et technologies. YX and Y. Hu are supported by the National Natural Science Foundation of China (41025018) and by the National Basic Research Program of China (973 Program, 2010CB428606). SWS is supported by Korea Ministry of Environment as “Climate Change Correspondence Program”. We acknowledge the World Climate Research Programme's Working Group on Coupled Modelling for the CMIP5 model data used in this study.

References

Butchart, N., and Coauthors, 2006: Simulations of anthropogenic change in the strength of the Brewer–Dobson circulation. Climate Dyn., 27, 727–741, doi:10.1007/s00382-006-0162-4.

Bunzel, F., and H. Schmidt, 2013: The Brewer-Dobson circulation in a changing climate: Impact of the model configuration. Journal of the Atmospheric Sciences, 70(9), 3002-3002.

Dessler, A. E., Schoeberl, M. R., Wang, T., Davis, S. M., & Rosenlof, K. H. , 2013, Stratospheric water vapor feedback. *Proceedings of the National Academy of Sciences*, *110*(45), 18087-18091.

Dessler, A. E., M. R. Schoeberl, T. Wang, S. M. Davis, K. H. Rosenlof, *and* J.-P. Vernier, 2014, Variations of stratospheric water vapor over the past three decades, J. Geophys. Res. Atmos., 119, 12,588–12,598, *doi:*10.1002/2014JD021712.

Forster, P. M. D. and K. P. Shine, 1999. "Stratospheric water vapour changes as a possible contributor to observed stratospheric cooling." Geophysical Research Letters 26(21): 3309-3312.

Fueglistaler, S., et al., 2014, Departure from Clausius-Clapeyron scaling of water entering the stratosphere in response to changes in tropical upwelling, J. Geophys. Res. Atmos., 119, 1962–1972, *doi:*10.1002/2013JD020772.

Gerber et al., 2012: Assessing and understanding the impact of stratospheric dynamics and variability on the earth system. Bull. Amer. Meteor. Soc., 93, 845–859.

Gettelman, A., *et al.* , 2010, Multimodel assessment of the upper troposphere and lower stratosphere: Tropics and global trends, J. Geophys. Res., 115, *D00M08, doi:*10.1029/2009JD013638.

Hansen, J., M. Sato, and R. Ruedy, 1997: Radiative forcing and climate response. *J. Geophys. Res. Atmos.,* **102**, 6831-6864.

Hegglin, M. I., Tegtmeier, S., Anderson, J., Froidevaux, L., Fuller, R., Funke, B., ... & Weigel, K., 2013, SPARC Data Initiative: Comparison of water vapor climatologies from international satellite limb sounders. *Journal of Geophysical Research: Atmospheres*, *118*(20), 11-824.

Huang, Y., V. Ramaswamy, and B. Soden, 2007:An investigation of the sensitivity of the clear-sky outgoing longwave radiation to atmospheric temperature and water vapor, J. Geophys. Res., 112, D05104,doi:10.1029/2005JD006906.

Huang, Y., 2013a: A simulated climatology of spectrally decomposed atmospheric infrared radiation, J. of Climate, doi: 10.1175/JCLI-D-12-00438.1.

Huang, Y., 2013b: On the Longwave Climate Feedbacks. Journal of Climate 26(19): 7603-7610.

Huang, Y. and M. Zhang, 2014: The implication of radiative forcing and feedback for meridional energy transport, Geophys. Res. Lett., DOI: 10.1002/2013GL059079.

Joshi, M. M., M. J. Webb, et al., 2010. "Stratospheric water vapour and high climate sensitivity in a version of the HadSM3 climate model." Atmospheric Chemistry and Physics 10(15): 7161-7167.

Li, F., J. Austin, and R. J. Wilson, 2008:The strength of the Brewer-Dobson circulation in a changing climate: coupled chemistry-climate model simulations, J. Clim., 21, 40-57.

Manzini, E., et al., 2014:Northern winter climate change: Assessment of uncertainty in CMIP5 projections related to stratosphere-troposphere coupling, J. Geophys. Res. Atmos., 119, doi:10.1002/2013JD021403.

McClatchey, R. A., R. W. Fenn, J. E. Selby, F. E. Volz, and J. S. Garing, 1972:Optical Properties of the Atmosphere, Third Edition, Air 599 Force Geophysical Laboratory Technical Report, AFCRL-72-0497, 80 pp.

McLandress, C., and T. G. Shepherd, 2009: Simulated Anthropogenic Changes in the Brewer–Dobson Circulation, Including Its Extension to High Latitudes. J. Climate, 22, 1516–1540. doi: 10.1175/2008JCLI2679.1

Mote, P. W., K. H. Rosenlof, et al., 1996. "An atmospheric tape recorder: The imprint of tropical tropopause temperatures on stratospheric water vapor." Journal of Geophysical Research 101(D2): 3989.

Neale, R. B., and Coauthors, 2010: Description of the NCAR Community Atmosphere Model (CAM5.0). NCAR Tech. Rep. NCAR/TN-486+STR, 268 pp.

Shell, K. M., J. T. Kiehl, et al., 2008: "Using the radiative kernel technique to calculate climate feedbacks in NCAR's Community Atmospheric Model." Journal of Climate 21(10): 2269-2282.

Shepherd, T. G., and C. McLandress, 2011: A robust mechanism for strengthening of the brewer–dobson circulation in response to climate change: critical-layer control of subtropical wave breaking. J. Atmos. Sci., 68, 784–797. doi: 10.1175/2010JAS3608.1

Brian J. Soden and Isaac M. Held, 2006: An Assessment of Climate Feedbacks in Coupled Ocean–Atmosphere Models. *J. Climate*, **19**, 3354–3360.

Soden, B. J., I. M. Held, R. Colman, K. M. Shell, J. T. Kiehl, and C. A. Shields, 2008:Quantifying climate feedbacks using radiative kernels. *J. Clim.*, **21**, 3504-3520.

Son, S.-W., L. M. Polvani, et al., 2009. "The Impact of Stratospheric Ozone Recovery on Tropopause Height Trends." Journal of Climate 22(2): 429-445.

Stuber, N., M. Ponater, et al., 2001. "Is the climate sensitivity to ozone perturbations enhanced by stratospheric water vapor feedback?" Geophysical Research Letters 28(15): 2887-2890.

Taylor, K. E., R. J. Stouffer, et al., 2011. "An Overview of CMIP5 and the Experiment Design." Bulletin of the American Meteorological Society 93(4): 485-498.

WMO, 1957: Definition of the tropopause. *WMO Bull.,* **6**, 136.

Zelinka, M., et al., 2012: Computing and Partitioning Cloud Feedbacks Using Cloud Property Histograms. Part I: Cloud Radiative Kernels, J. Climate, 25, 3715–3735, doi:10.1175/JCLI-D-11-00248.1.

Zhang, M., Y. Huang, 2014: Radiative forcing of quadrupling CO_2, J. Climate, doi: http://dx.doi.org/10.1175/JCLI-D-13-00535.1.

Zhou, C., A. E. Dessler, M. D. Zelinka, P. Yang, and T. Wang, 2014: Cirrus feedback on interannual climate fluctuations, Geophys. Res. Lett., 41, doi:10.1002/2014GL062095.

Tables

Table 1. Stratospheric temperature and water vapor feedback parameters of each model in the unit of W m^{-2} K^{-1}. Two methods are used here: a differencing method and a regression method (see details in the texts). The results are grouped to high-top (HT, at 1 hPa or above) and low-top (LT) models. See Table 9.A.1 of the IPCC 5th assessment report for details of the models.

MODEL	Model top	Differencing Method			Regression Method		
		λ_{Tst}	λ_{WVst}	λ_{st}	λ_{Tst}	λ_{WVst}	λ_{st}
GFDL-CM3	HT	-0.02	0.03	0.01	-0.02	0.03	0.01
IPSL-CM5A-LR	HT	0.04	0.03	0.07	0.06	0.02	0.08
MPI-ESM-MR	HT	0.01	0.03	0.03	0.01	0.02	0.03
MRI-CGCM3	HT	-0.09	0.03	-0.06	-0.07	0.03	-0.04
CanESM2	HT	-0.03	0.03	-0.01	-0.03	0.02	-0.01
CCSM4	LT	-0.06	0.01	-0.05	0.00	0.01	0.01
CSIRO-Mk3.6.0	LT	0.03	0.01	0.04	0.04	0.00	0.04
HadGEM2-ES	LT	0.02	0.02	0.04	0.06	0.02	0.07
INMCM4	LT	-0.03	0.01	-0.01	-0.02	0.02	0.00
MIROC5	LT	-0.02	0.01	-0.01	-0.01	0.02	0.01
NorESM1-M	LT	-0.01	0.01	-0.00	0.01	0.01	0.02
Mean		-0.02	0.02	0.00	0.01	0.02	0.02
STD		0.04	0.01	0.04	0.04	0.01	0.04

Table 2. Correlation between global mean lowermost (below 70hPa) and overworld (above 70hPa) stratospheric specific humidity and two control factors: temperature at the cold point tropopause (CPT) averaged over 10°S–10°N and tropical upper tropospheric specific humidity (UTH) averaged over 30°S–30°N. The correlation coefficients are calculated based on the annual mean anomalies of these variables in Years 21-150 in the abrupt 4xCO2 experiment for each model. In the case of CPT+UTH, stratospheric specific humidity is first regressed to the two variables in a multiple regression and then correlation coefficient is calculated between GCM-simulated and regression-model-predicted humidity anomalies.

MODEL	Model top	Lowermost stratosphere			Overworld stratosphere		
		CPT + UTH	CPT	UTH	CPT + UTH	CPT	UTH
GFDL-CM3	HT	0.99	-0.07	0.99	0.92	0.13	0.89
IPSL-CM5A-LR	HT	0.99	-0.33	0.99	0.91	-0.30	0.91
MPI-ESM-MR	HT	0.99	-0.25	0.99	0.87	0.18	0.77
MRI-CGCM3	HT	0.97	0.92	0.97	0.87	0.83	0.87
CanESM2	HT	0.99	-0.06	0.99	0.86	0.01	0.86
CCSM4	LT	0.97	0.26	0.97	0.86	0.32	0.86
CSIRO-Mk3.6.0	LT	0.99	0.94	0.99	0.96	0.92	0.95
HadGEM2-ES	LT	0.98	-0.97	0.98	0.95	-0.91	0.95
INMCM4	LT	0.91	0.34	0.91	0.37	-0.05	0.36
MIROC5	LT	0.98	0.95	0.97	0.75	0.72	-0.57
NorESM1-M	LT	0.97	0.39	0.97	0.85	0.40	0.85

Figures

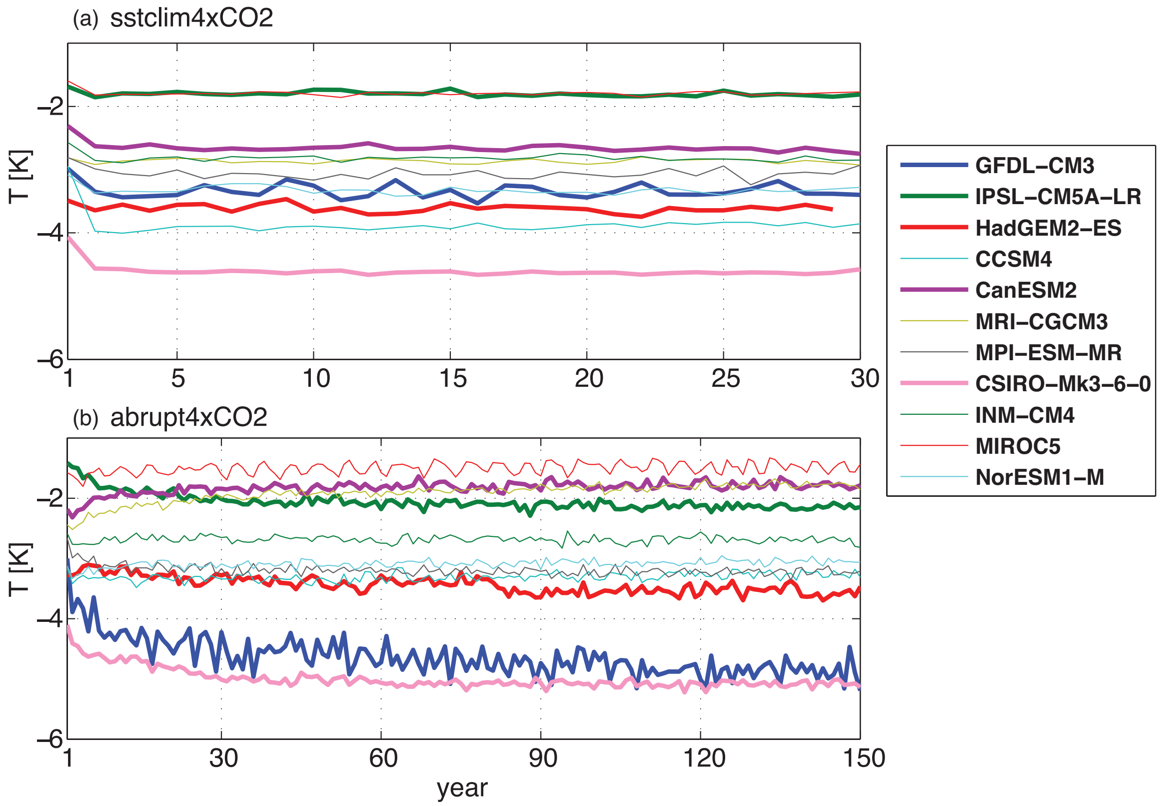

Figure 1. Time series of global mean 50 hPa temperature change in the sstClim4xCO2 (top) and abrup4xCO2 (bottom) experiments. The changes (unit: K) are relative to their control runs sstClim and piControl, respectively. Note that the range of x-axis is different in two time series.

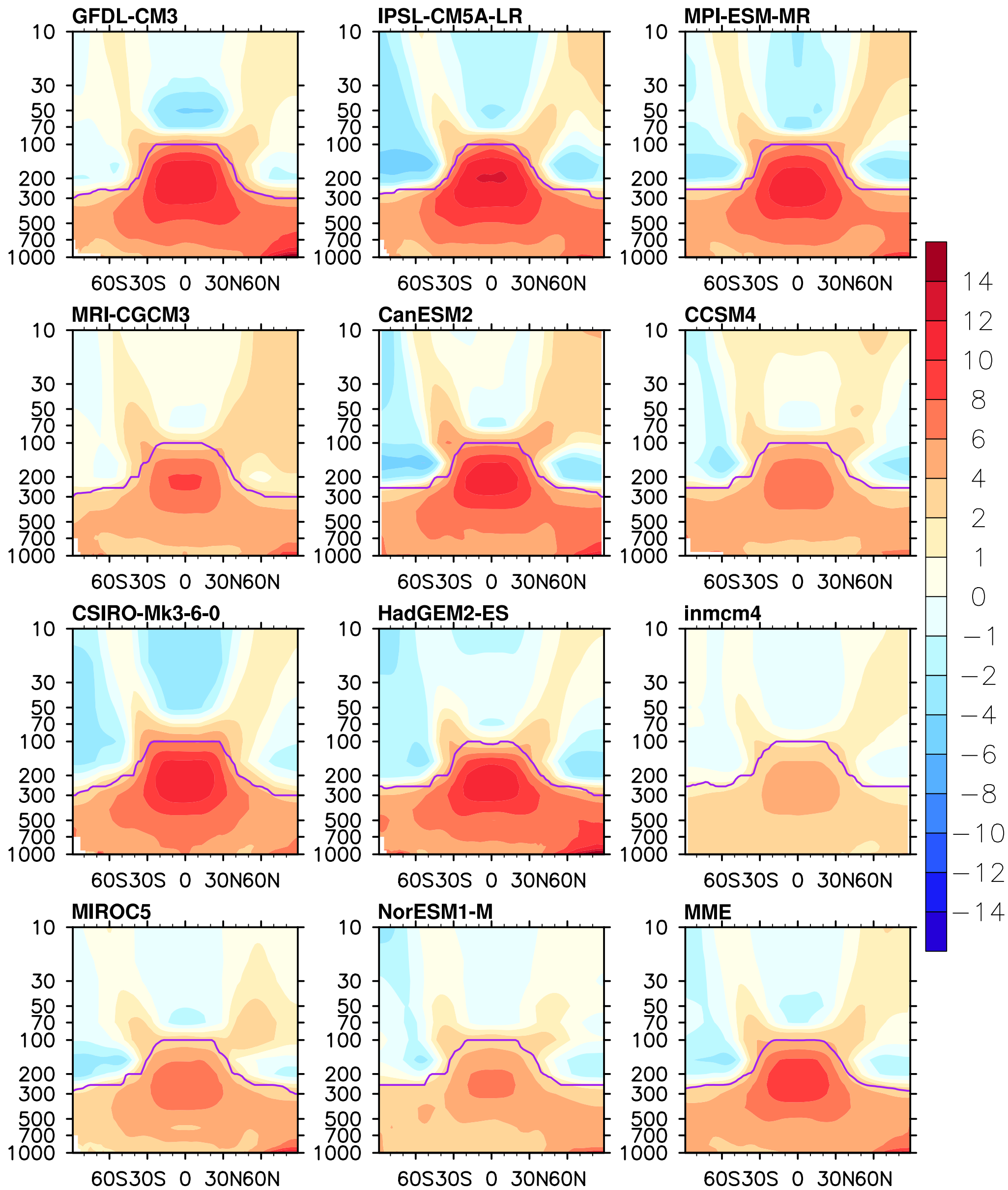

Figure 2. Zonal mean feedback response in a) atmospheric temperature ΔT, unit: K, and b) logarithm of specific humidity, $\Delta\log_2(q)$. The thick line indicates the tropopause.

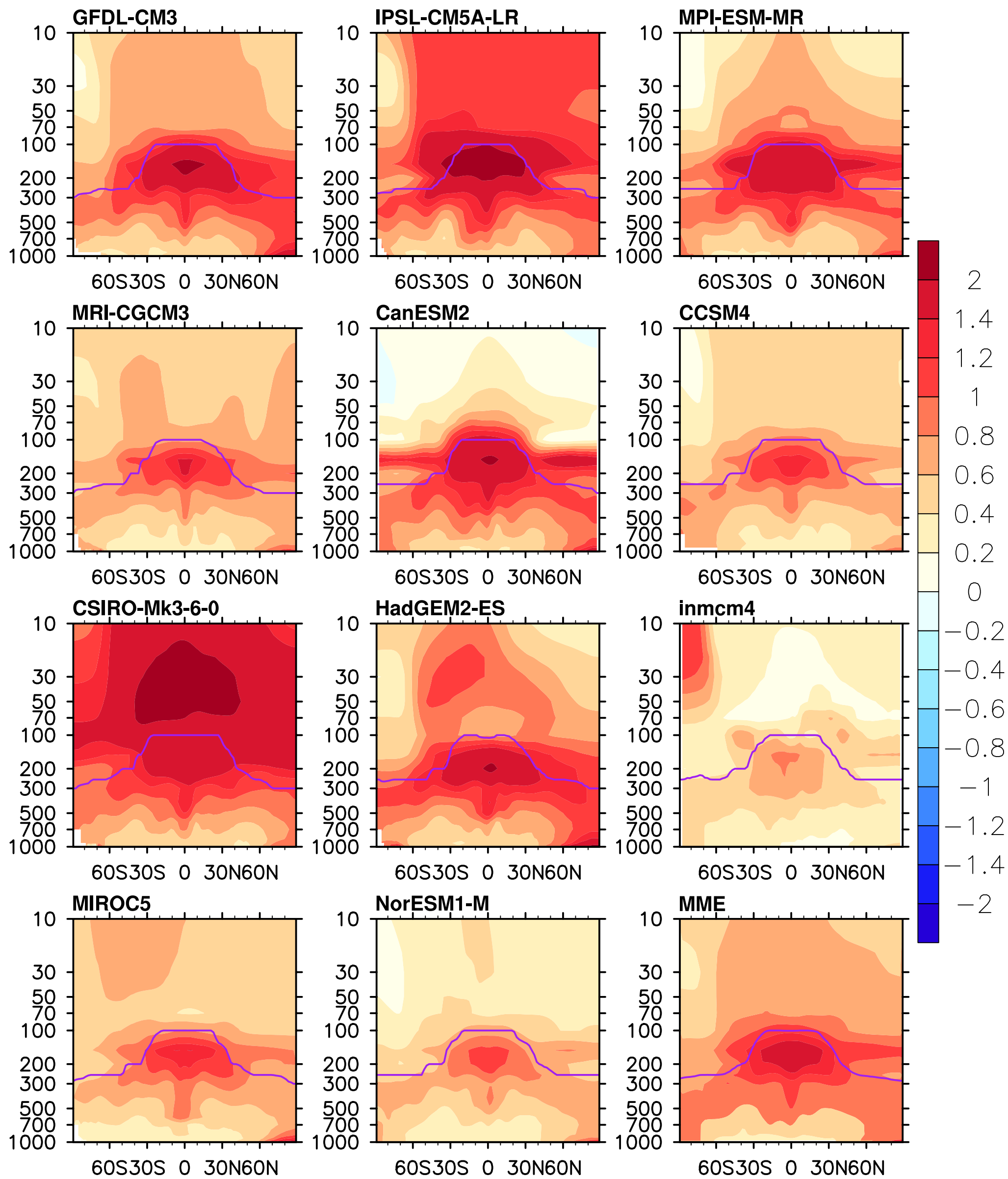

Figure 2 b. Zonal mean feedback response in the logarithm of specific humidity, $\Delta\log_2(q)$.

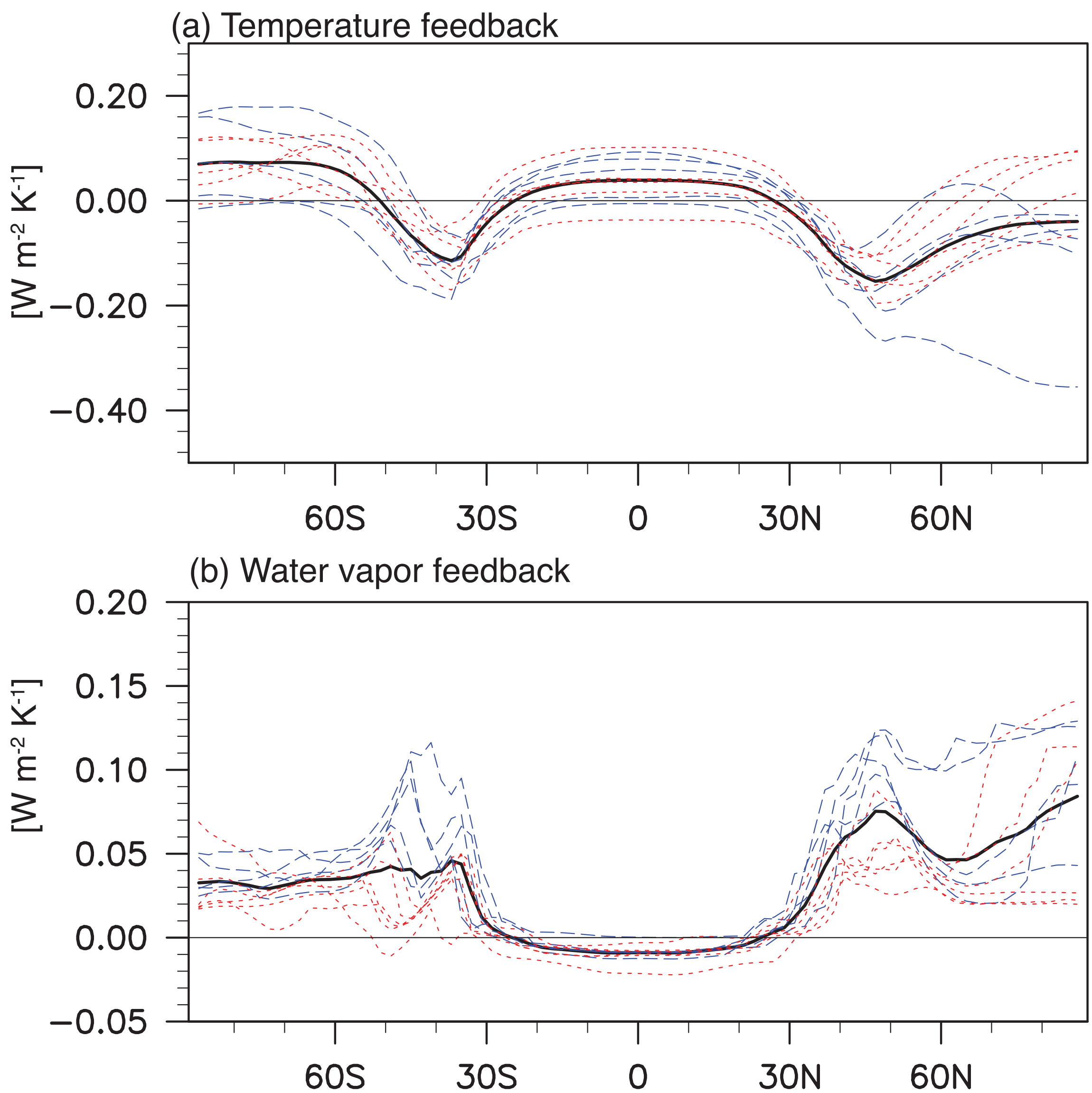

Figure 3. Zonal mean radiative feedbacks (unit: $W\ m^{-2}\ K^{-1}$) of the stratospheric a) temperature and b) water vapor. The high- and low-top models are denoted by blue and red dashed lines respectively. The thick black line denotes the multi-model mean.

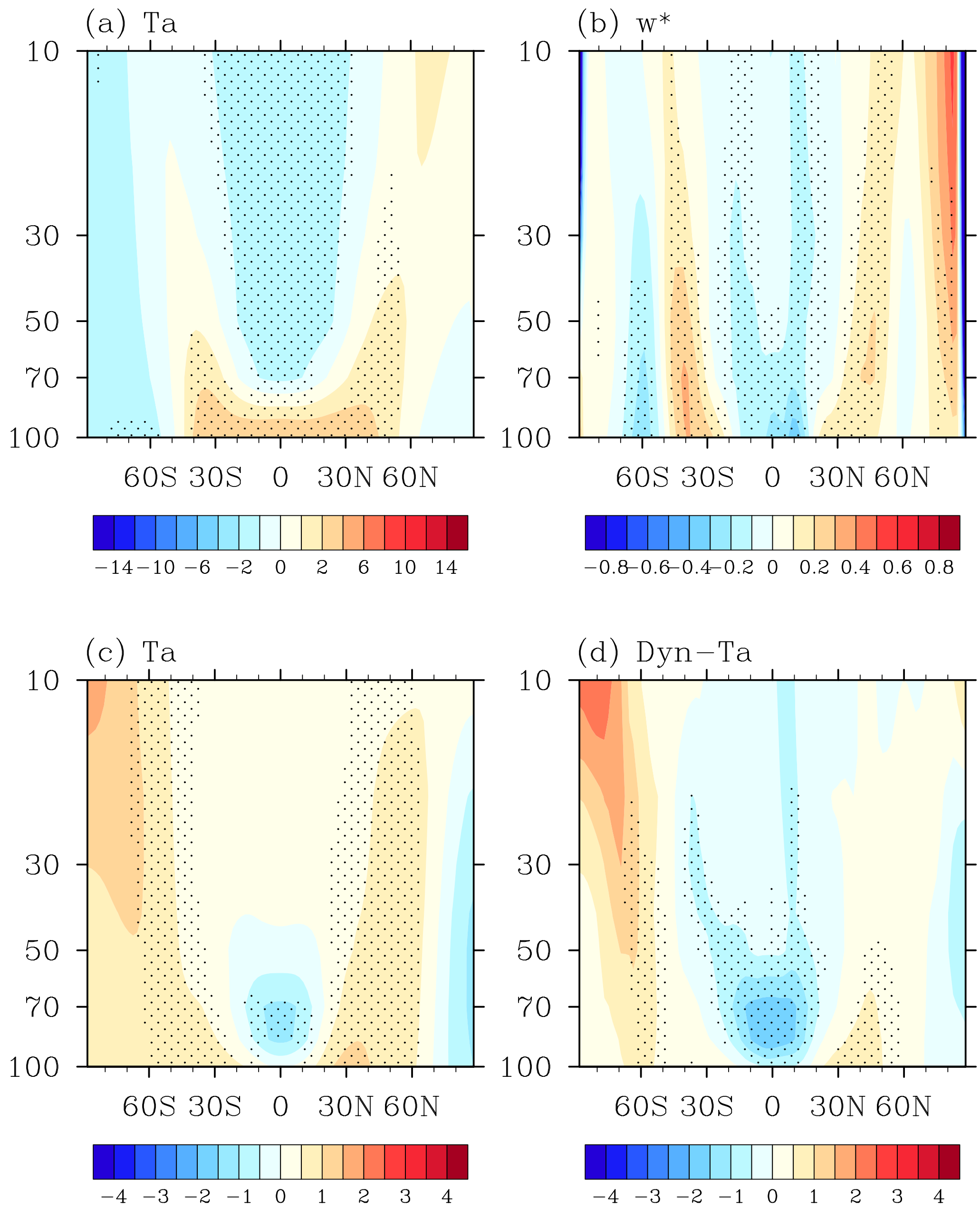

Figure 4. a) Multi-model mean feedback temperature response (unit: K) in the abrupt4xCO_2 experiment. b) Multi-model mean change in the residual vertical velocity w^*

of the overturning circulation in the abrupt4xCO_2 experiment (unit: mm/s). Contoured here is $(-1)\times\Delta w^{*}$, so that negative (positive) means ascent (descent). c) The ensemble mean feedback temperature response (unit: K) in the CAM5 experiment. d) The dynamics contribution to the temperature response (unit: K) in c). For the CAM5 experiment, the change is the difference between the means of 2003-2007 and 1960-1964. In (a) and (b), stippling indicates at least 13 models showing the same sign of change; in (c) and (d), significant trend at 90% confidence level.